

# Limited Compatibility of Polymerase Subunit Interactions in Influenza A and B Viruses<sup>\*[5]</sup>

Received for publication, January 9, 2010, and in revised form, March 31, 2010. Published, JBC Papers in Press, April 2, 2010, DOI 10.1074/jbc.M110.102533

Kerstin Wunderlich<sup>†§¶</sup>, Mindaugas Juozapaitis<sup>||</sup>, Benjamin Mänz<sup>‡</sup>, Daniel Mayer<sup>‡</sup>, Veronika Götz<sup>‡</sup>, Andrea Zöhner<sup>\*\*</sup>, Thorsten Wolff<sup>\*\*</sup>, Martin Schwemmler<sup>‡2</sup>, and Arnold Martin<sup>‡</sup>

From the <sup>‡</sup>Department of Virology, <sup>§</sup>Spemann Graduate School of Biology and Medicine, and <sup>¶</sup>Faculty of Biology, University of Freiburg, 70104 Freiburg, Germany, the <sup>||</sup>Institute of Biotechnology, LT-02241 Vilnius, Lithuania, and the <sup>\*\*</sup>Robert Koch-Institut, D-13353 Berlin, Germany

Despite their close phylogenetic relationship, natural intertypic reassortants between influenza A (FluA) and B (FluB) viruses have not been described. Inefficient polymerase assembly of the three polymerase subunits may contribute to this incompatibility, especially because the known protein-protein interaction domains, including the PA-binding domain of PB1, are highly conserved for each virus type. Here we show that substitution of the FluA PA-binding domain (PB1-A<sub>1–25</sub>) with that of FluB (PB1-B<sub>1–25</sub>) is accompanied by reduced polymerase activity and viral growth of FluA. Consistent with these findings, surface plasmon resonance spectroscopy measurements revealed that PA of FluA exhibits impaired affinity to biotinylated PB1-B<sub>1–25</sub> peptides. PA of FluB showed no detectable affinity to biotinylated PB1-A<sub>1–25</sub> peptides. Consequently, FluB PB1 harboring the PA-binding domain of FluA (PB1-AB) failed to assemble with PA and PB2 into an active polymerase complex. To regain functionality, we used a single amino acid substitution (T6Y) known to confer binding to PA of both virus types, which restored polymerase complex formation but surprisingly not polymerase activity for FluB. Taken together, our results demonstrate that the conserved virus type-specific PA-binding domains differ in their affinity to PA and thus might contribute to intertypic exclusion of reassortants between FluA and FluB viruses.

Influenza A and B viruses are closely related RNA viruses that cause respiratory disease. Although influenza A viruses (FluA) infect both humans and a broad variety of animals, influenza B viruses (FluB) are predominantly restricted to humans (1). Both viruses co-circulate in the human population and cause significant morbidity and mortality. Although FluB viruses usually show a lower prevalence of human infections, in some influenza seasons, they account for the majority of cases (1–4).

Correct assembly of the heterotrimeric polymerase complex consisting of the subunits PA, PB1, and PB2 is essential for

transcription and replication of influenza viruses in the nucleus of infected cells. Direct biochemical interactions have been shown for PB1 and PB2 as well as for PA and PB1 (5–9), whereas a weak transient interaction has been proposed for PA and PB2 (10). For FluA, it was demonstrated that PB1 possesses the RNA polymerization activity, whereas PB2 is able to bind specifically to host-derived capped mRNA, which is subsequently cleaved off by the PA endonuclease (11–13). It is assumed that the polymerase subunits of FluA and FluB share similar if not identical functions.

Despite their close phylogenetic relationship, intertypic reassortants between FluA and FluB viruses have not been described (14–16). The reasons for this are not fully understood. There is evidence for a preferential virus type-specific recognition of viral promoter regions, which might contribute to the lack of such reassortants due to growth disadvantages (17, 18). This impairment in viral growth was first observed with a FluA chimera containing a neuraminidase gene harboring FluB 5'- and 3'-non-coding regions (18). In addition, combinations of FluA and FluB polymerase subunits fail to support polymerase activity (19–21). This could be caused by an incompatibility of the enzymatic functions of the heterologous polymerase subunits. Additionally, assembly of the heterotrimeric polymerase complex could be prevented by type-specific protein-protein interaction domains including the well characterized PA-binding domain of PB1 (5, 6, 22). A  $3_{10}$ -helix within the N-terminal 25 amino acids of PB1 (PB1<sub>1–25</sub>) is critical for binding of the virus polymerase subunits PB1 to PA (23, 24). This domain is highly conserved in a virus type-specific manner (see Fig. 1A) (22). In addition, these subtype-specific differences correlate with the observations that FluA and FluB PA-binding peptides bind efficiently to the homologous but not to the heterologous PA subunit (22). Accordingly, peptides derived from the first 25 amino acids of FluA PB1 are able to inhibit the polymerase activity of FluA but not FluB and vice versa (22). We could recently show that the virus type-specific affinity of the FluA PA-binding peptide can be converted into a dual binding affinity by a single FluB-specific substitution of threonine to tyrosine at amino acid position 6 (22). This peptide binds to PA of both virus types and exhibits antiviral activity against FluA and FluB. However, the effect of this single aa<sup>3</sup> substitution in

\* This work was supported by grants from the Deutsche Forschungsgemeinschaft, the European Commission's Seventh Framework, and FluResearchNet.

[5] The on-line version of this article (available at <http://www.jbc.org>) contains supplemental Figs. 1S–3S and Table S1.

<sup>1</sup> Supported by the Excellence Initiative of the German Research Foundation (GSC-4, Spemann Graduate School).

<sup>2</sup> To whom correspondence should be addressed: Hermann-Herder Str. 11, 70104 Freiburg, Germany. Tel.: 49-7612036526; Fax: 40-7612036639; E-mail: martin.schwemmler@uniklinik-freiburg.de.

<sup>3</sup> The abbreviations used are: aa, amino acids; HA, hemagglutinin; MDCK, Madin-Darby canine kidney cells; SPR, surface plasmon resonance; WT, wild type; m.o.i., multiplicity of infection; vRNA, viral RNA.

the context of full-length PB1 on polymerase activity and viral growth remains to be shown.

Here we provide evidence that the PA-binding domains of FluA and FluB are not exchangeable between virus types without a decrease in polymerase activity. Furthermore, the dual PA-binding domain inserted into PB1 of FluA and FluB cannot overcome this incompatibility for FluB. Biochemical binding studies further indicate that FluA and FluB differ in their PA binding affinities. Finally, we provide evidence that not only decreased but also increased affinity of this binding site correlates with reduced polymerase activity and viral growth.

## EXPERIMENTAL PROCEDURES

**Plasmids**—To obtain the pHW2000 vector containing segment 2 coding for the various PB1 chimeras, QuikChange site-directed mutagenesis (Stratagene) was carried out on pHW2000-PB1-Lee or pHW2000-PB1-SC35M, respectively (25, 26), resulting in plasmids pHW2000-PB1-AT6Y, pHW2000-PB1-AB, pHW2000-PB1-AT6YB, and pHW2000-PB1-BA. The expression plasmids pCAGGs-PA-A/B-HIS and pCAGGs-PB1-A/B-HA were described elsewhere (22). Plasmids pCAGGs-PB1-BA-HA, -PB1-AT6YB-HA, and -PB1-AT6Y-HA were created by assembly PCR from the respective FluA SC35M and FluB Lee genes, cloned into the EcoRI/XmaI sites (for constructs based on the C-terminal open reading frame of FluA) or NotI/XmaI (FluB) opened pCAGGs vector containing an HA tag after the XmaI site. In analogy, pCAGGs-PB2-A-FLAG was obtained by inserting the PB2 open reading frame of SC35M into an EcoRI/XmaI opened FLAG tag-harboring pCAGGs plasmid.

To obtain chimera expression plasmids, which were tested in minireplicon assays (see Fig. 5), an EcoRI/EcoRV fragment of pCAGGs-PB1-AT6YB was subcloned into a pBS-KSII(+) vector, where QuikChange site-directed mutagenesis was performed. After PCR, the mutated sequence was reintroduced by cloning the respective mutated EcoRI/EcoRV fragment back into the pCAGGs background. All expression plasmids were sequenced to guarantee correctness of the used constructs.

**Cells and Viruses**—293T and MDCK II cells were grown in Dulbecco's modified Eagle's medium supplemented with 10% fetal calf serum, 2 mM L-glutamine, and antibiotics. All cells were maintained at 37 °C and 5% CO<sub>2</sub>. Infection experiments were carried out using recombinant A/SC35M (H7N7) and B/Lee/40 and the indicated mutant viruses A/SC35M-PB1-AT6Y, A/SC35M-PB1-BA, and B/Lee/40-PB1-AT6Y B. The recombinant WT influenza B/Lee/40 and SC35M have been described elsewhere (25, 26).

Yeast *Saccharomyces cerevisiae* 214Δpep4 MATa (*ura3 leu2 his3 Δpep4*) was used for the expression of PA proteins. Transformation and subsequent selection were carried out as described (27). For protein expression, yeast cells were inoculated into selective YEPD and grown for 24 h at 28 °C; thereafter yeast cells were reinoculated into YEPG induction medium and cultured further for 24 h at 28 °C.

**Virus Infections and Growth Assays**—MDCK II cells were infected at a multiplicity of infection (m.o.i.) of 0.001 at 37 °C for A/SC35M, A/SC35M-PB1 AT6Y, and A/SC35M PB1-BA and at 33 °C for B/Lee/40 and B/Lee/40-PB1-AT6YB. Virus

titers were determined at the indicated time points by plaque assay for SC35M and expressed as plaque-forming units/ml. FluB/Lee/40 virus titers were determined by indirect immunofluorescence staining and were expressed as fluorescence-forming units/ml as described elsewhere (25).

**Purification of Recombinant PAs**—To prevent proteolysis, all manipulations were carried out at 4 °C. Yeast cells were harvested by centrifugation at 800 × g for 5 min and resuspended in disruption buffer (20 mM Na<sub>2</sub>HPO<sub>4</sub>, pH 8.0, 300 mM NaCl, 20 mM imidazole, 10% isopropyl alcohol, 2 mM phenylmethylsulfonyl fluoride). Complete protease inhibitor mixture tablets (Roche Applied Science) were added to the disruption buffer (1 tablet/20 g of wet yeast biomass). Cells were cyclically disrupted after mixing 12 times with glass beads (Sigma) in a blender at 3,000 rpm for 12 min. After centrifugation at 3,500 × g for 10 min, PA proteins containing supernatant were filtered through a 0.45-μm membrane (Millipore), mixed with nickel-nitrilotriacetic acid agarose (Qiagen), which was previously equilibrated in binding buffer (20 mM Na<sub>2</sub>HPO<sub>4</sub>, pH 8.0, 300 mM NaCl, 20 mM imidazole), and incubated for 40 min in batch mode. Thereafter the resin was loaded into the column and washed with 5 column volumes of binding buffer, with 5 column volumes of first wash solution 1 (20 mM Na<sub>2</sub>HPO<sub>4</sub>, pH 7.4, 500 mM NaCl, 20 mM imidazole, 2% Tween 20, 1% glycerol), and finally with 5 column volumes of second wash solution 2 (20 mM Na<sub>2</sub>HPO<sub>4</sub>, pH 7.4, 300 mM NaCl, 20 mM imidazole). Recombinant PAs were eluted with elution buffer (20 mM Na<sub>2</sub>HPO<sub>4</sub>, pH 7.4, 300 mM NaCl, and 250 mM imidazole) in a one-step gradient. Highest PA concentrations containing fractions were pooled, and imidazole was removed during a desalting step using Millipore ultrafiltration device.

**Surface Plasmon Resonance Analysis**—All interaction studies were performed in real time with a Biacore 3000 system (GE Healthcare). The experiments were done at 25 °C at a flow rate of 30 μl min<sup>-1</sup> in Tris-based buffer (25 mM Tris, pH 7.4, 150 mM NaCl, 0.01% surfactant). Peptides containing the N-terminal 25 amino acids of PB1 and a C-terminally fused biotin tag were immobilized on a streptavidin chip. A scrambled control peptide was used (which contained the same amino acids as PB1 but in a random order) (22). Association (1 min) of the purified, recombinant PA proteins was followed by a 2-min dissociation phase during which the used buffer was perfused. For analysis of the affinity constants, various concentrations of the analyte were injected. To regenerate the chip, the bound protein was removed by a 10-s pulse of 50 mM NaOH. The obtained data were analyzed with the BIAevaluation 3.1 evaluation software using the 1:1 Langmuir binding model for calculation of association and dissociation rate constants ( $K_{on}$  and  $K_{off}$ ) and the dissociation equilibrium constants ( $K_D = K_{off}/K_{on}$ ).

**Co-immunoprecipitation and Immunoblot Analysis**—293T cells were transfected with the indicated plasmids in 6-well plates using METAFECTENE (Biontix, Martinsried, Germany). Cells were incubated 24 h after transfection with lysis buffer (20 mM Tris, pH 7.5, 100 mM NaCl, 0.5 mM EDTA, 0.5% Nonidet P-40, 1% protease inhibitor mix G (Serva, Heidelberg, Germany), 1 mM dithiothreitol) for 15 min on ice. After centrifugation by 13,000 rpm at 4 °C, supernatant was incubated with anti-HA-specific (Sigma) or FLAG M2-specific antibodies

## Influenza Polymerase Complex Formation

(Sigma) coupled to agarose beads, respectively, for 1 h at 4 °C. After three washes with 1 ml of washing buffer (lysis buffer without protease inhibitor mix), bound material was eluted under denaturing conditions, separated on SDS-PAGE gels, and transferred to polyvinylidene difluoride membranes. Viral polymerase subunits were detected with antibodies directed against the HA (Covance, Berkeley, CA), His (Qiagen), or FLAG tag (Sigma).

**Reconstitution of the Influenza Virus Polymerase Activity**—The experiments were essentially carried out as described (28). Briefly, 293T cells were transiently transfected with a plasmid mixture containing either FluA or FluB PB1, PB2, or PA (45 ng of each) or NP expression plasmids (150 ng) and a polymerase I expression plasmid (25 ng) expressing an influenza virus-like RNA coding for the reporter protein firefly luciferase to monitor viral polymerase activity. Both minigenome RNAs were flanked by non-coding sequences of segment 8 of FluA and FluB, respectively. The transfection mixture also contained a plasmid constitutively expressing *Renilla* luciferase (20 ng), which served to normalize variation in transfection efficiency. For the determination of the FluB/Lee/40 polymerase activity, 293T cells were transfected with the Pol1/Pol2 expression plasmids coding for PB1, PA, PB2 (50 ng of each), and NP (100 ng) and pPol-B/NS-Luc (125 ng) encoding a firefly luciferase cDNA of negative polarity flanked by the non-coding regions of the viral NS segment. The constitutive expression vector pTK-RL (Promega) was used to normalize for transfection efficiency (5 ng).

**Virus Rescue and Growth of Influenza A and B Viruses**—For FluA virus rescue, confluent 293T cells in six-well tissue culture plates were transfected with a mixture of the eight pHW2000 plasmids (300 ng of each), the four pCAGGS plasmids (150 ng of each) coding for PA, PB1, PB2, and NP, and Lipofectamine 2000 (Invitrogen) according to the manufacturer's instructions. Six hours later, the DNA transfection mixture was replaced by infection medium (Dulbecco's modified Eagle's medium + 1% penicillin/streptomycin + 0.2% bovine serum albumin + 1% glutamine). Two days after transfection, 200  $\mu$ l of the supernatant was added to confluent MDCK II cells. Rescued viruses were plaque-purified, and MDCK II cells were infected for propagation of stock virus. The influenza B mutant virus B/Lee PB1-A6YT-B was generated by transfecting 293T cells with a pHW2000-based plasmid as described elsewhere (29). At 72 h after transfection, the supernatant was inoculated into the allantoic cavities of 10-day-old embryonated chicken eggs, and stock of recombinant virus was grown for 3 days at 33 °C (29). The presence of the introduced mutations within the PB1 sequence was confirmed by cycle sequencing of amplified reverse transcription-PCR product.

**Primer Extension Analysis**—Cells were infected with SC35M at an m.o.i. of 2 and harvested 6 h after infection. Total RNA was isolated using TRIzol reagent (Invitrogen). After spectrophotometric quantification and normalization, RNA primer extensions were carried out as described previously (30–32), with minor modifications. Briefly, 2 pmol of DNA primer was 5'-end labeled with [<sup>32</sup>P]ATP using T4 polynucleotide kinase, and it was mixed with 1  $\mu$ g of total RNA in 6  $\mu$ l of water and denatured at 95 °C for 3 min. The mixture was then cooled on ice,

and reverse transcriptase SuperScript II (Invitrogen) and its reaction buffer were added. Primer extensions were performed at 45 °C for 1 h. The NP and NA primers described in Ref. 33 were used. Transcription products were analyzed on 6% polyacrylamide gels containing 7 M urea in Tris-borate-EDTA buffer and detected by autoradiography. Transcription products were quantified using Fuji MacBas v2.2 software.

**qPCR Analysis of Packaged vRNAs**—To analyze packaged vRNAs, virus stocks were prepared and adjusted to equal HA titers. Viral RNA was isolated using the QiaAMP viral RNA mini kit (Qiagen) and reverse transcribed (QuantiTect reverse transcription kit (Qiagen)), and reverse transcriptase products were used for quantitative PCR analysis. Separate PCRs were carried out with segment-specific primers and probes ([supplemental Table S1](#)) by use of a LightCycler 1.5 (Roche Applied Science) using a QuantiFast probe kit (Qiagen).

Relative concentrations of vRNA were determined by analysis of cycle threshold values, normalizing for the total vRNA amount by equalizing the levels of NS vRNA and then calculating the percentage of incorporation relative to the levels of WT RNA packaging. Results are presented as the average incorporations of vRNA  $\pm$  S.D., with results derived from two independent virus stocks.

## RESULTS

**The PA-binding Domains of PB1 from FluA and FluB Show Limited Compatibility due to a Different Binding Affinity Profile**—To test whether the PA-binding domains of PB1 are exchangeable between FluA and FluB, we generated PB1 chimeras using the strains A/SC35M and B/Yamagata/73. The chimeras contained the PA-binding domain from one virus type and the rest of the protein from the other virus type, designated PB1-AB and PB1-BA (Fig. 1A). Co-immunoprecipitation studies using cell extracts of transiently transfected 293T cells revealed efficient dimer formation between PB1-AB and FluA PA (PA-A) as well as between PB1-BA and FluB PA (PA-B) (Fig. 1B), confirming that PB1<sub>1–25</sub> mediates type-specific binding to PA (22). However, neither PB1-BA nor PB1-AB bound to PA-A or PA-B, respectively (Fig. 1B, lanes 2 and 5), indicating that the PA-binding domains are not mutually exchangeable without significant loss of dimer formation.

Surprisingly, despite inefficient dimer formation, PB1-BA retained 70% of its polymerase activity in a FluA minireplicon system, which is the reconstitution of the viral ribonucleoprotein complex and a reporter gene in human cells (Fig. 1C). In contrast, PB1-AB was inactive. This correlated with the ability of PB1-BA to form a trimeric polymerase complex, whereas PB1-AB failed to associate with PA-A and PB2-A (Fig. 1D, lanes 2 and 3), indicating an incompatibility of PB2-A and PB1-AB. Lack of trimer formation was accompanied by reduced levels of PB2-A (Fig. 1D, lanes 3 and 4, and data not shown), which is most likely the result of enhanced degradation of unbound PB2-A.

In contrast to the FluA polymerase activity observed with PB1-BA, the PB1-AB chimera exhibited no detectable FluB polymerase activity, (Fig. 1E), which is reflected by the inability of this chimera to assemble with PA-B and PB2-B into a polymerase complex (Fig. 1F). In conclusion, trimer formation was

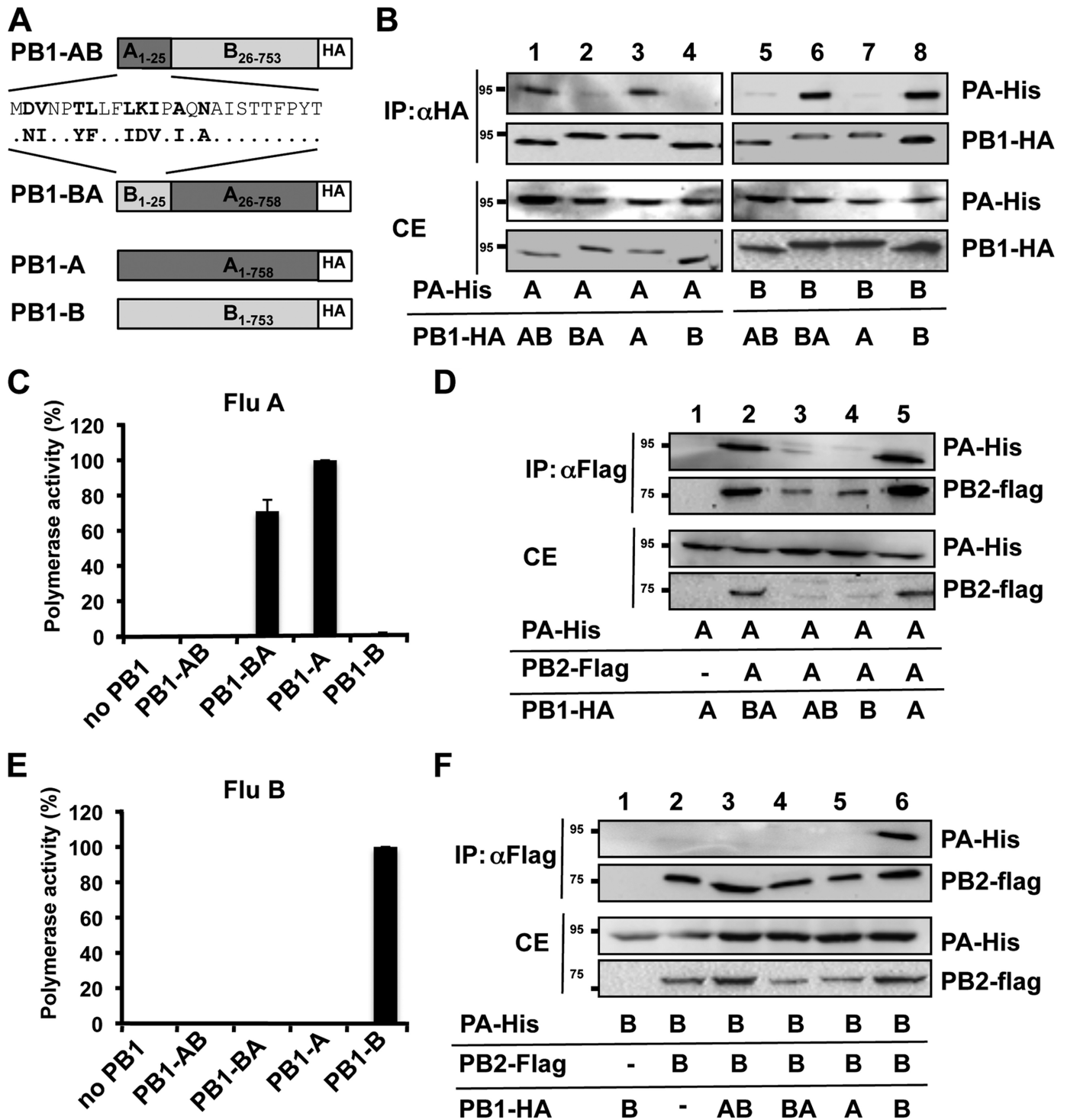


**FIGURE 1. Mutual exchange of the PA-binding domains of FluA and FluB affects assembly and polymerase activity.** *A*, schematic depicting the PB1 chimeras used in *B–F*. PB1-AB and PB1-BA represent fusion proteins containing the PA-binding domain of FluA or FluB (aa 1–25) and the heterologous portion of FluB (aa 26–753) and FluA PB1 (aa 26–758), respectively. *B*, dimer formation by FluA PA and the indicated PB1 chimeras. Human 293T cells were transiently transfected with His-tagged PA (*PA-His*) and HA-tagged PB1 chimeras (*PB1-HA*) and subjected to co-immunoprecipitations (*IP*) using HA-specific antibodies. Precipitated polymerase subunits were identified by Western blot analysis using specific antibodies against the HA and His tag. *CE*, cell extract. *C*, determination of the FluA polymerase activity of the PB1 chimeras. The activity observed with PB1-A was set to 100%. The omission of PB1 (*no PB1*) in the transfection mixture served as a negative control. *D*, trimer formation of FluA polymerase complex in the presence of the indicated PB1 chimeras. 293T cells were transiently transfected with His-tagged PA (*PA-His*), HA-tagged PB1 chimeras and FLAG-tagged PB2 (*PB2-flag*), and subjected to co-immunoprecipitations using FLAG-specific antibodies. *E*, determination of the FluB polymerase activity of the PB1 chimeras. The experiments were essentially carried out as described in *C* using FluB polymerase subunits and a FluB-specific reporter construct expressing *Renilla luciferase*. Error bars in *C* and *E* indicate S.D. *F*, trimer formation of the FluB polymerase complex in the presence of the indicated PB1 chimeras was essentially carried out as described in *D* using FluB-specific subunits.

## Influenza Polymerase Complex Formation

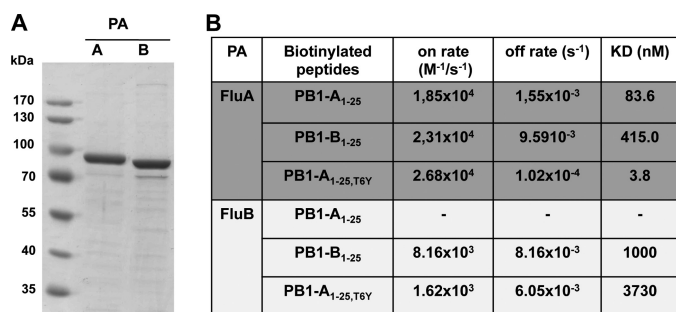


**FIGURE 2. Determination of the PA binding affinities of different PB1<sub>1-25</sub> peptides.** A, purification of FluA and FluB PA from yeast. C-terminally His-tagged PAs from FluA (A/SC35M) or FluB (B/Yamagata) were expressed in yeast, purified from the soluble fraction by nickel-agarose, and analyzed for their purity by SDS-PAGE and subsequent staining with Coomassie Blue. B, binding kinetics between His-PA and the indicated biotinylated peptides were determined by SPR.

a prerequisite for polymerase function, whereas efficient dimer formation between PA and PB1 was not required.

Because PB1-BA supported FluA polymerase activity despite inefficient dimer formation with PA-A in our co-immunoprecipitation experiments, we used surface plasmon resonance spectroscopy (SPR) to gain further insight into the nature of the PB1-PA binding characteristics. On/off rates and dissociation constants ( $K_D$ ) between C-terminally biotinylated peptides comprising the PA-binding domain of either FluA PB1 (PB1-A<sub>1-25</sub>) or FluB PB1 (PB1-B<sub>1-25</sub>) and purified His-tagged PA of both virus types were determined (Fig. 2A). The SPR measurements for FluA PA revealed  $K_D$  values of 83.6 nM for the interaction with PB1-A<sub>1-25</sub> and 415 nM with PB1-B<sub>1-25</sub> (Fig. 2B). The 5-fold difference in the  $K_D$  values is mainly caused by a higher off rate of PA-A from PB1-B<sub>1-25</sub> (Fig. 2B). An even higher  $K_D$  of 1,000 nM was determined for the binding between PA-B and PB1-B<sub>1-25</sub>. Consistent with the lack of trimer formation, no specific binding of PB1-A<sub>1-25</sub> to PA-B was detectable.

In summary, despite the inability of PB1-BA to form a stable dimer with PA-A, there apparently exists sufficient affinity of PB1-B<sub>1-25</sub> to PA-A to allow stable trimeric complex formation and polymerase activity. Furthermore, the lack of any detectable binding between PB1-A<sub>1-25</sub> to PA-B is consistent with the inability of PB1-AB to assemble into a functional FluB polymerase complex.

**The Dual PA-binding Domain Supports Polymerase Activity in FluA but Not in FluB despite Efficient Trimeric Polymerase Complex Formation**—We recently showed that a FluA-derived peptide, designated PB1<sub>1-25,T6Y</sub>, with a single aa substitution T6Y, efficiently binds to PA of various FluA and FluB strains (22). We therefore reasoned that this PA-binding domain introduced into full-length PB1-A (PB1-A<sub>T6Y</sub>) and PB1-B (PB1-A<sub>T6Y</sub>B) (Fig. 3A) should result in the formation of an active polymerase complex in both virus types. When tested for dimer formation, both chimeras, PB1-A<sub>T6Y</sub> and PB1-A<sub>T6Y</sub>B, efficiently co-immunoprecipitated PA of both FluA and of FluB (Fig. 3B), confirming the dual binding activity of PB1<sub>1-25</sub>A<sub>T6Y</sub> in the context of a full-length PB1 protein.

In the minireplicon assay, PB1-A<sub>T6Y</sub> supported FluA polymerase activity, although with reduced efficiency as compared with PB1-A (Fig. 3C), which correlated with trimeric polymerase formation (Fig. 3D, lane 4). However, PB1-A<sub>T6Y</sub>B

only showed polymerase activity below 1% as compared with PB1-B in the FluB replicon assay (Fig. 3E). Intriguingly, despite the lack of polymerase activity of PB1-A<sub>T6Y</sub>B, polymerase complex assembly with PA-B and PB2-B was not affected (Fig. 3F, lane 3).

Our co-immunoprecipitation studies did not reveal differences in the ability of PB1-A<sub>T6Y</sub> and PB1-A<sub>T6Y</sub>B to assemble into trimeric FluA and FluB polymerase complexes, respectively. However, the polymerase activity was negatively affected in both cases and may correlate with altered PA binding affinities. Determination of the binding kinetics by SPR revealed a higher  $K_D$  value for the interaction of PA-B to PB1-A<sub>1-25,T6Y</sub> as compared with PB1-B<sub>1-25</sub> (Fig. 2B). In contrast, as compared with PB1-A<sub>1-25</sub>, we determined a 22-fold lower  $K_D$  for the interaction between PA-A and PB1-A<sub>1-25,T6Y</sub>. Overall, these results indicate that decreased as well as increased PA binding affinities prevent optimal polymerase activity.

To evaluate the impact of the PB1 chimeras in the context of recombinant viruses, we rescued FluA (A/SC35M) coding for PB1-BA or PB1-A<sub>T6Y</sub> and FluB (B/Lee/40) coding for PB1-AB or PB1-A<sub>T6Y</sub>B. Determination of the polymerase activity with PB1-A<sub>T6Y</sub>B in the B/Lee/40 background revealed similarly reduced polymerase activity of less than 3% of wild-type activity (supplemental Fig. 1S). With the exception of the FluB mutant expressing PB1-AB, all viruses could be rescued (Fig. 4). As compared with WT virus, A/SC35M-PB1-BA showed an impaired growth on MDCK II cells of 2 log<sub>10</sub> 24 h after infection with an m.o.i. of 0.001 and did not reach WT levels at later time points. SC35M-PB1-A<sub>T6Y</sub> replicated ~20-fold less efficiently at early time points after infection but reached WT levels after 24 h (Fig. 4A). In contrast, B/Lee/40 PB1-A<sub>T6Y</sub>B was severely attenuated by almost 5 log<sub>10</sub> (Fig. 4B). Overall, the extent of reduced viral growth caused by the PB1 chimeras is comparable with the reduced polymerase activity measured in the minireplicon.

The nucleotide changes in the PB1 gene of the FluA mutant viruses coding for the PA-binding region overlap with known genome packaging signals (34). To evaluate whether genome packaging is affected, we determined the ratios of the NS, PA, and PB1 genomes in stock viruses by quantitative reverse transcription-PCR and normalization for the total vRNA amount by equalization of the level of NS vRNA. This analysis revealed no significant difference in the ratios of these incorporated genome segments between WT and A/SC35M PB1-A<sub>T6Y</sub> (supplemental Fig. 2S), indicating that packaging is not responsible for the attenuation of this virus. However, levels of PA and PB1 were decreased in virus particles of A/SC35M PB1-BA by 38 and 75%, which suggests that inefficient packaging of viral genomes also contributed to the impaired viral growth of this mutant virus.

To analyze whether viral transcription or replication or both are affected in cells infected with the FluA mutants, we compared the ratios of viral RNA transcripts (vRNAs, cRNA, and mRNA). For this purpose, MDCK cells were infected with either WT or mutant FluA viruses with an m.o.i. of 2 for 6 h, and total RNA was prepared and subjected to primer extension analysis. The ratios between viral transcripts in either WT or mutant virus in infected cells were comparable, although the

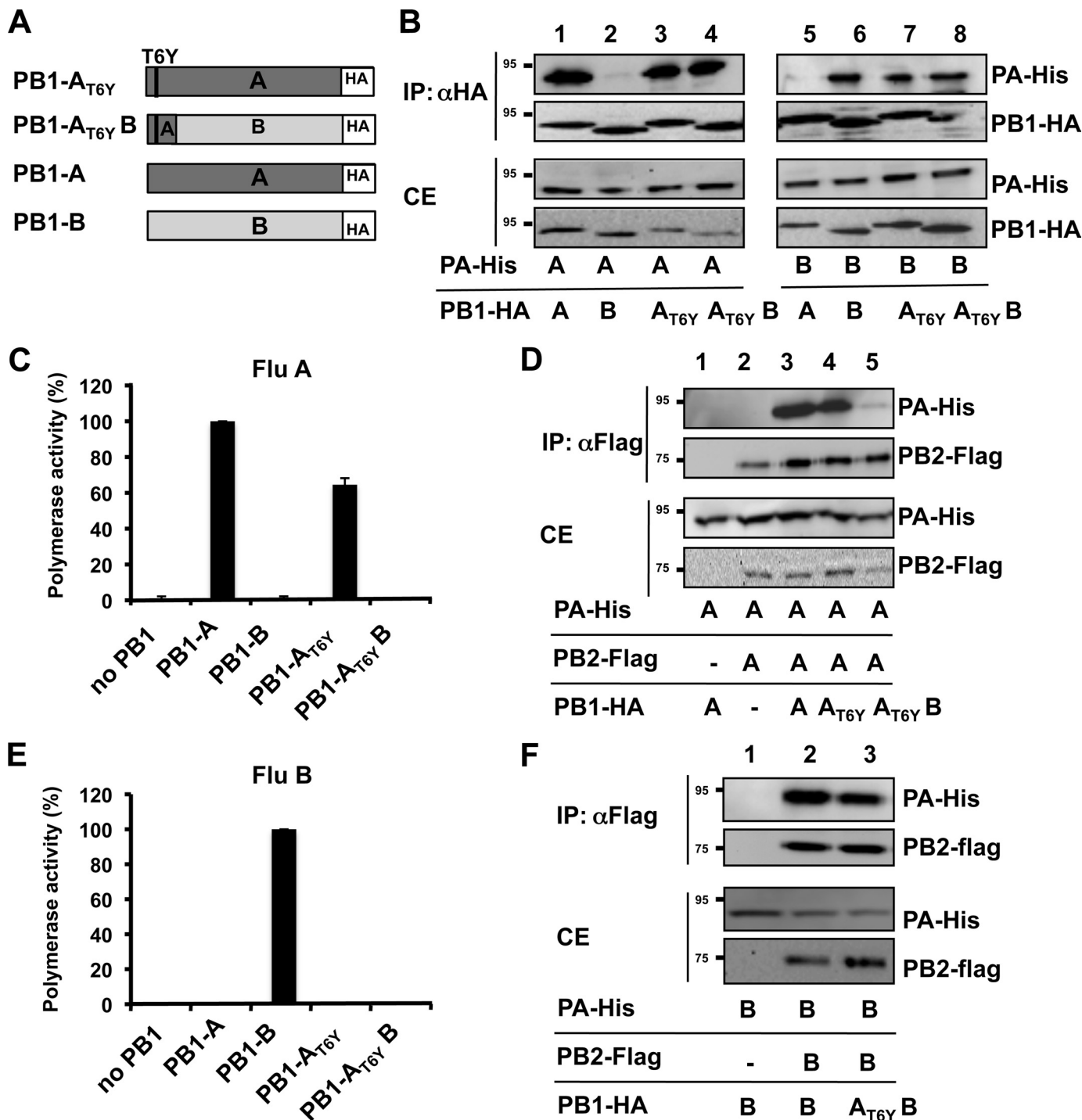


**FIGURE 3. Polymerase activity of PB1 chimeras harboring the dual PA-binding domain.** *A*, schematic depicting the PB1 chimeras used in *B–F* including a fusion protein consisting of the PA-binding domain of FluA (aa 1–25) harboring the FluB-specific threonine to tyrosine substitution at aa position 6 and the heterologous portion of FluB (aa 26–753). *B*, dimer formation of FluA and FluB (PA-His) and the indicated HA-tagged PB1 chimera. *IP*, immunoprecipitations; *CE*, cell extract. *C*, determination of the FluA polymerase activity of the indicated PB1 chimeras was carried out as described in the legend for Fig. 1*C*. *D*, trimer formation of FluB polymerase complex in the presence of the indicated PB1 chimeras as in Fig. 1*D*. *E*, determination of the FluA polymerase activity of the PB1 chimeras. The experiments were essentially carried out as described in the legend for Fig. 1*C*. *Error bars* in *C* and *E* indicate S.D. *F*, trimer formation of the FluA polymerase complex in the presence of the indicated PB1 chimeras was essentially carried out as described in *D* using FluB-specific subunits.

overall levels of viral transcripts were slightly lower in cells infected with the FluA mutants (supplemental Fig. 3S). Taken together, these results indicate that the polymerase of both mutant viruses causes a general decline of all viral transcripts.

*The Majority of the Conserved Amino Acids of the FluB PA-binding Domain Are Required to Support FluB Polymerase*

*Activity*—PB1-A<sub>T6Y</sub>B possessed strongly diminished polymerase activity in the FluB minireplicon (Fig. 3*E*), indicating that further FluB-specific amino acids are required to restore WT polymerase activity. The crystal structure of FluA PB1 (aa 1–16) and the C-terminal part of PA (PDB ID: 2ZNL) revealed that a 3<sub>10</sub>-helix comprising aa 5–11 (PTLLFLK, Fig. 5*A*) is critical for

## Influenza Polymerase Complex Formation

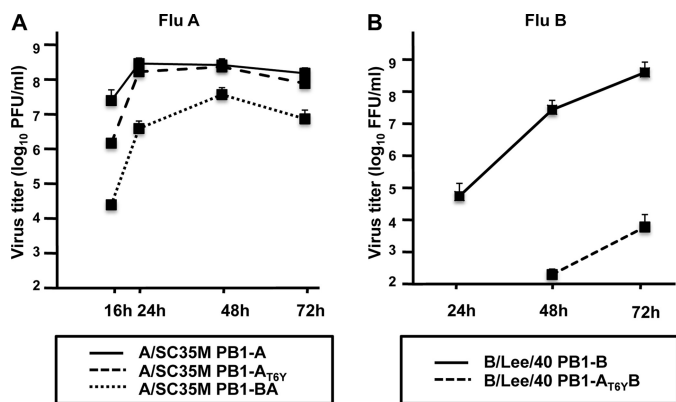


**FIGURE 4. Viral growth of FluA and FluB mutant viruses.** MDCK cells were infected with the indicated FluA viruses expressing PB1-A (A/SC35M PB1-A), PB1-A<sub>T6Y</sub> (A/SC35M PB1-A<sub>T6Y</sub>), PB1-BA (A/SC35M PB1-BA) (A) or FluB viruses expressing WT PB1-B (B/Lee/40 PB1-B) or PB1-B harboring the dual PA-binding domain (B/Lee/40 PB1-A<sub>T6Y</sub>B) (B) at an m.o.i. of 0.001. Error bars represent S.D. from three independent experiments. PFU, plaque-forming units; FFU, fluorescence-forming units.

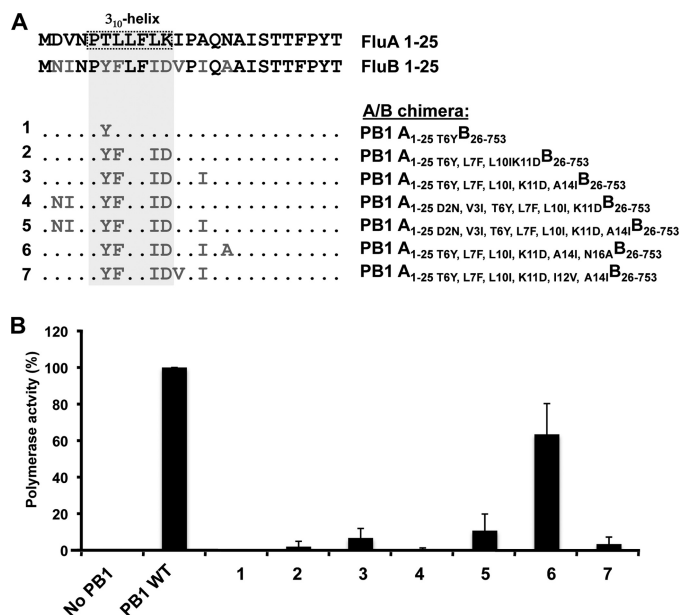


**FIGURE 5. Polymerase activity of PB1-A<sub>T6Y</sub>B chimeras harboring additional FluB-specific amino acid substitutions in the PA-binding domain.** A, upper panel, alignment of the consensus sequence of the FluB and FluA PA-binding domain (aa 1–25). Type-specific amino acids are highlighted in bold. Lower panel, PB1-AB chimeras harboring additional FluB-specific amino acids (highlighted in gray). The 3<sub>10</sub>-helix in the FluA PA-binding domain is indicated by a dashed box. B, determination of the FluB polymerase activity of the HA-tagged PB1 chimeras depicted in A. The experiments were essentially carried out as described in the legend for Fig. 1C. Error bars indicate S.D.

binding to PA (23, 24). To restore PB1-A<sub>T6Y</sub>B to near WT activity, aa 7, 10, and 11 in this helix were therefore substituted with FluB-specific aa (Fig. 5A). This chimera, designated PB1-A<sub>T6Y,L7F,L10I,K11D</sub>B, was 33-fold more active than PB1-A<sub>T6Y</sub>B; however, as compared with WT PB1-B, the polymerase activity was still below 2% (Fig. 5B). An additional substitution of aa 14 (PB1-A<sub>T6Y,L7F,L10I,K11D,A14I</sub>B) further enhanced the activity to 7%. In contrast, the PB1 chimera harboring the FluB-specific aa of the core-binding region and aa 14 and 16 (PB1-A<sub>T6Y,L7F,L10I,K11D,A14I,N16A</sub>B) showed activity above 70% (Fig. 5B). Thus, although the FluA polymerase complex tolerated up to 9 FluB-specific aa in the PA-binding domain, the FluB

polymerase complex appears to tolerate only 3 FluA-specific aa in the same domain. This highlights the difference in tolerance of amino acid substitutions between FluA and FluB polymerases.

## DISCUSSION

We recently showed that peptides derived from the PA-binding domains of FluA or FluB block the viral polymerase activity in a virus type-specific manner (22, 28). Accordingly, enzyme-linked immunosorbent assay-based binding assays revealed that these peptides only bind efficiently to the subtype-specific PA (22). Based on these results, we hypothesized that intertypic exchange of this binding site between FluA and FluB would not lead to a functional trimeric polymerase complex.

Here we show that substitution of the PA-binding domains causes impaired polymerase activity and viral growth. Complete loss of PA binding affinity as measured by SPR for PA-binding domain of PB1-A, and its failure to bind to PA-B prevents trimeric polymerase complex formation and the generation of viable FluB viruses harboring this domain. Surprisingly, although the FluB PB1 chimera harboring the dual PA-binding domain assembled efficiently with FluB PB2 and PA into trimeric polymerase complexes, only residual polymerase activity was observed. In line with these observations, FluB viruses expressing this PB1 chimera showed severely reduced viral growth. Vice versa, the PA-binding domain of FluB PB1 is able to bind to FluA PA, although with reduced affinity, resulting in reduced polymerase activity and viral growth.

We assume that impaired viral growth of the FluA mutant viruses coding for the PB1-BA is also caused by impaired genome packaging because we observed reduced levels of viral polymerase gene segments in virus preparations. Although little is known about packaging signals of FluB viruses, we speculate that this also applies for the FluB mutant virus studied in this work.

It was shown that a deletion of the PA-binding domain of PB1 prevents dimer formation with PA (5). However, although dimer formation between PB1-BA and FluA PA was also negatively affected, formation of the trimeric polymerase complex was not impaired. We therefore suggest that the addition of PB2, which weakly interacts with PA (10), compensates for the strongly diminished PA binding affinity of PB1-B<sub>1–25</sub> and is sufficient to promote trimer assembly and polymerase activity. On the other hand, the PB1 chimera PB1-AB harboring the PA-binding domain of FluA forms a complex with PA-A, but further assembly into trimers is very inefficient. Thus, it seems likely that other protein interaction domains such as the PB1-PB2 interaction domain bind in a subtype-specific manner and might therefore additionally contribute to the incompatibility of the polymerase complexes between FluA and FluB. Indeed, the PB1-binding domain of PB2 appears to be conserved in a virus type-specific manner (data not shown). Furthermore, the contribution of C-terminal PB1 domains to PA binding has not been fully characterized.

The virus type-specific conservation of the PA-binding domain is most likely the consequence of an independent evolution of the FluA and FluB strains resulting in the fixation of

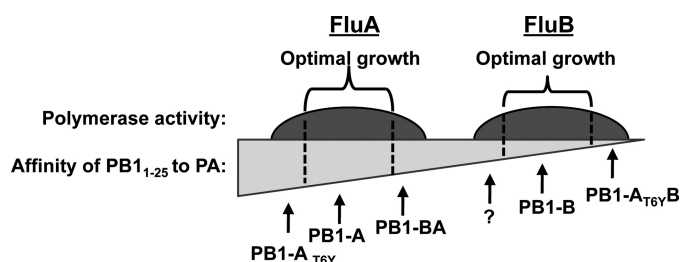


**FIGURE 6. Model of the interrelationship between optimal growth of FluA and FluB viruses and PA binding affinities.** Within a certain range of PA binding affinity (between *dashed lines*), optimal polymerase activity is ensured. However, FluA and FluB acquired substantially different PA binding affinities during independent evolution, resulting in a limited compatibility of the PA-binding domains between virus types. Lower, but also higher, PA binding affinities result in impaired polymerase activity as exemplified by the indicated PB1 mutants. The *question mark* indicates that FluB PB1 mutants that exhibit higher PA binding affinities and show impaired polymerase activity are not described yet. For further details, see under “Discussion.”

subtype-specific aa and PA binding affinities. Because reassortment is essential for influenza virus subtypes to allow adaptation to new hosts (1), there is most likely a selection against unfavorable PA binding affinities that would result in impaired polymerase activity.

Several lines of evidence suggest that only within a certain range of PA binding affinities, efficient polymerase activity and viral growth are achieved, and that this optimal range differs between FluA and FluB (Fig. 6). First, we could show that the FluA and FluB PB1 N termini have acquired substantially different PA binding affinities, resulting in a 10-fold lower affinity between PA and PB1<sub>1-25</sub> of FluB and FluA, respectively (Fig. 2). Secondly, we provide evidence that reduction in PA affinity results in impaired polymerase activity; PB1-BA showed 30% impairment in a FluA polymerase assay, and the activity of PB1-A<sub>T6Y</sub>B was even below 1% of WT FluB polymerase activity. The pronounced inactivity of PB1-A<sub>T6Y</sub>B in the FluB minireplicon is most likely due to the very low affinity of the PA-binding domain (Fig. 6). Thirdly, as exemplified by PB1-A<sub>T6Y</sub>, we could also show that enhanced PA binding affinities reduce the polymerase activity (Fig. 3). Thus, variations from the optimal affinity are only partially tolerated (Fig. 6). In general, FluB seems to be more affected by changes in PB1<sub>1-25</sub> due to the already lower affinity of the PA-binding domain of PB1-B. Whether increased PA binding affinities might also reduce polymerase activity of FluB as predicted in our model (Fig. 6) remains to be shown. As demonstrated earlier, substitutions with FluA-specific aa residues did not result in enhanced binding to FluB PA (22).

This interdependence between efficient polymerase activity and optimal affinity to PA appears to be independent of the formation of the trimeric polymerase. PB1-A<sub>T6Y</sub>B efficiently assembled with PA-B and PB2-B in a co-immunoprecipitation experiment, albeit the polymerase activity of this complex was very low. Likewise, PB1-A<sub>T6Y</sub> assembled efficiently with PA-A and PB2-A but also revealed impaired polymerase activity as compared with WT PB1-A. It therefore seems possible that the interaction between PB1 and PA has to retain a certain degree of flexibility after formation of the trimeric complex. Indeed, extensive structural rearrangements occur after binding of the polymerase complex to the viral ribonucleoprotein (1, 35, 36).

Hence, it is possible that the PA-PB1 interaction has to be transiently released or requires a certain degree of flexibility during those rearrangements. Too low or too high PA binding affinities might therefore interfere with dynamic structural changes. In addition, further rearrangements of the viral polymerase complex during transcription and replication may require a transient release of protein-protein interactions within the trimeric polymerase complex, including the PA-binding domain of PB1.

In summary, our results indicate that the type-specific conservation of the PA-binding domains of PB1 resulted in a functional incompatibility that contributes to the exclusion of naturally occurring intertypic reassortants between FluA and FluB viruses.

*Acknowledgments*—We thank Geoffrey Chase, Georg Kochs, and Friedemann Weber for critical reading of the manuscript, Stefan Höhnig for help with the SPR measurements, and Anna Överby and Marcus Panning for support in the quantitative real-time-PCR studies.

## REFERENCES

- Chen, R., and Holmes, E. C. (2008) *J. Mol. Evol.* **66**, 655–663
- Baine, W. B., Luby, J. P., and Martin, S. M. (1980) *Am. J. Med.* **68**, 181–189
- Kim, H. W., Brandt, C. D., Arrobio, J. O., Murphy, B., Chanock, R. M., and Parrott, R. H. (1979) *Am. J. Epidemiol.* **109**, 464–479
- Nolan, T. F., Jr., Goodman, R. A., Hinman, A. R., Noble, G. R., Kendal, A. P., and Thacker, S. B. (1980) *J. Infect. Dis.* **142**, 360–362
- Perez, D. R., and Donis, R. O. (2001) *J. Virol.* **75**, 8127–8136
- Pérez, D. R., and Donis, R. O. (1995) *J. Virol.* **69**, 6932–6939
- Ohtsu, Y., Honda, Y., Sakata, Y., Kato, H., and Toyoda, T. (2002) *Microbiol. Immunol.* **46**, 167–175
- Biswas, S. K., and Nayak, D. P. (1996) *J. Virol.* **70**, 6716–6722
- Sugiyama, K., Obayashi, E., Kawaguchi, A., Suzuki, Y., Tame, J. R., Nagata, K., and Park, S. Y. (2009) *EMBO J.* **28**, 1803–1811
- Hemerka, J. N., Wang, D., Weng, Y., Lu, W., Kaushik, R. S., Jin, J., Harmon, A. F., and Li, F. (2009) *J. Virol.* **83**, 3944–3955
- Guilligay, D., Tarendeau, F., Resa-Infante, P., Coloma, R., Crepin, T., Sehr, P., Lewis, J., Ruigrok, R. W., Ortin, J., Hart, D. J., and Cusack, S. (2008) *Nat. Struct. Mol. Biol.* **15**, 500–506
- Yuan, P., Bartlam, M., Lou, Z., Chen, S., Zhou, J., He, X., Lv, Z., Ge, R., Li, X., Deng, T., Fodor, E., Rao, Z., and Liu, Y. (2009) *Nature* **458**, 909–913
- Dias, A., Bouvier, D., Crépin, T., McCarthy, A. A., Hart, D. J., Baudin, F., Cusack, S., and Ruigrok, R. W. (2009) *Nature* **458**, 914–918
- Tobita, K., Tanaka, T., Goto, H., and Feng, S. Y. (1983) *Arch. Virol.* **75**, 17–27
- Kaverin, N. V., Varich, N. L., Sklyanskaya, E. I., Amvrosieva, T. V., Petrik, J., and Vovk, T. C. (1983) *J. Gen. Virol.* **64**, 2139–2146
- Mikheeva, A., and Ghendon, Y. Z. (1982) *Arch. Virol.* **73**, 287–294
- Horimoto, T., Takada, A., Iwatsuki-Horimoto, K., Hatta, M., Goto, H., and Kawaoka, Y. (2003) *J. Virol.* **77**, 8031–8038
- Muster, T., Subbarao, E. K., Enami, M., Murphy, B. R., and Palese, P. (1991) *Proc. Natl. Acad. Sci. U.S.A.* **88**, 5177–5181
- Iwatsuki-Horimoto, K., Hatta, Y., Hatta, M., Muramoto, Y., Chen, H., Kawaoka, Y., and Horimoto, T. (2008) *Virus Res.* **135**, 161–165
- Crescenzo-Chaigne, B., Naffakh, N., and van der Werf, S. (1999) *Virology* **265**, 342–353
- Jambrina, E., Bárcena, J., Uez, O., and Portela, A. (1997) *Virology* **235**, 209–217
- Wunderlich, K., Mayer, D., Ranadheera, C., Holler, A. S., Mänz, B., Martin, A., Chase, G., Tegge, W., Frank, R., Kessler, U., and Schwemmler, M. (2009) *PLoS One* **4**, e7517
- He, X., Zhou, J., Bartlam, M., Zhang, R., Ma, J., Lou, Z., Li, X., Li, J., Joachimiak, A., Zeng, Z., Ge, R., Rao, Z., and Liu, Y. (2008) *Nature* **454**,



## Influenza Polymerase Complex Formation

- 1123–1126
24. Obayashi, E., Yoshida, H., Kawai, F., Shibayama, N., Kawaguchi, A., Nagata, K., Tame, J. R., and Park, S. Y. (2008) *Nature* **454**, 1127–1131
  25. Dauber, B., Schneider, J., and Wolff, T. (2006) *J. Virol.* **80**, 11667–11677
  26. Gabriel, G., Dauber, B., Wolff, T., Planz, O., Klenk, H. D., and Stech, J. (2005) *Proc. Natl. Acad. Sci. U.S.A.* **102**, 18590–18595
  27. Sasnauskas, K., Jomantiene, R., Lebediene, E., Lebedys, J., Januska, A., and Janulaitis, A. (1992) *Gene* **116**, 105–108
  28. Ghanem, A., Mayer, D., Chase, G., Tegge, W., Frank, R., Kochs, G., Garcia-Sastre, A., and Schwemmler, M. (2007) *J. Virol.* **81**, 7801–7804
  29. Dauber, B., Heins, G., and Wolff, T. (2004) *J. Virol.* **78**, 1865–1872
  30. Fodor, E., and Smith, M. (2004) *J. Virol.* **78**, 9144–9153
  31. Fodor, E., Crow, M., Mingay, L. J., Deng, T., Sharps, J., Fechter, P., and Brownlee, G. G. (2002) *J. Virol.* **76**, 8989–9001
  32. Gabriel, G., Abram, M., Keiner, B., Wagner, R., Klenk, H. D., and Stech, J. (2007) *J. Virol.* **81**, 9601–9604
  33. Gabriel, G., Nordmann, A., Stein, D. A., Iversen, P. L., and Klenk, H. D. (2008) *J. Gen. Virol.* **89**, 939–948
  34. Hutchinson, E. C., von Kirchbach, J. C., Gog, J. R., and Digard, P. (2010) *J. Gen. Virol.* **91**, 313–328
  35. Coloma, R., Valpuesta, J. M., Arranz, R., Carrascosa, J. L., Ortín, J., and Martín-Benito, J. (2009) *PLoS Pathog.* **5**, e1000491
  36. Torreira, E., Schoehn, G., Fernández, Y., Jorba, N., Ruigrok, R. W., Cusack, S., Ortín, J., and Llorca, O. (2007) *Nucleic Acids Res.* **35**, 3774–3783